Cooperative catalysis in a crystalline framework with templated acid–base sites

Devin S. Rollins,[a] Jackson Geary,[a] Kamaya Ronning,[a] Kathleen M. Snook,[a] and Dianne J. Xiao[a,*]

[a] Department of Chemistry, University of Washington, Seattle, Washington 98195-1700, United States.
*Corresponding author: djxiao@uw.edu

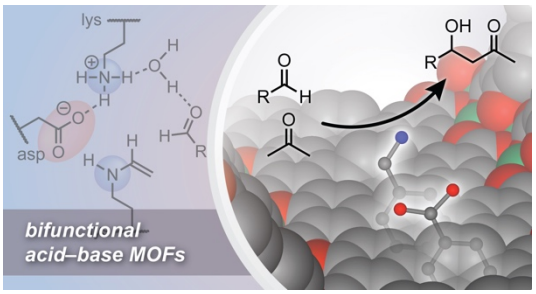

Abstract. Nature uses weakly basic residues in conjunction with weakly acidic residues to catalyze challenging heterolytic bond transformations. Here, we show that these cooperative effects can be replicated in a metal–organic framework containing bifunctional Brønsted acid–base sites. Using a templating strategy, we show, unambiguously, that the co-localization of acid and base sites is key to catalytic activity. Specifically, a thermolabile crosslinker containing tertiary ester and tertiary carbamate linkages is used to tether carboxylic acid and benzylamine pairs in close proximity during framework synthesis. These templated materials are over four-fold more active aldol condensation catalysts than non-templated materials containing randomly distributed acid and base sites. Together, this work establishes metal–organic frameworks as an exciting platform for cooperative acid–base catalysis that couples the advantages of heterogeneous catalysts with the structural precision of enzymes.

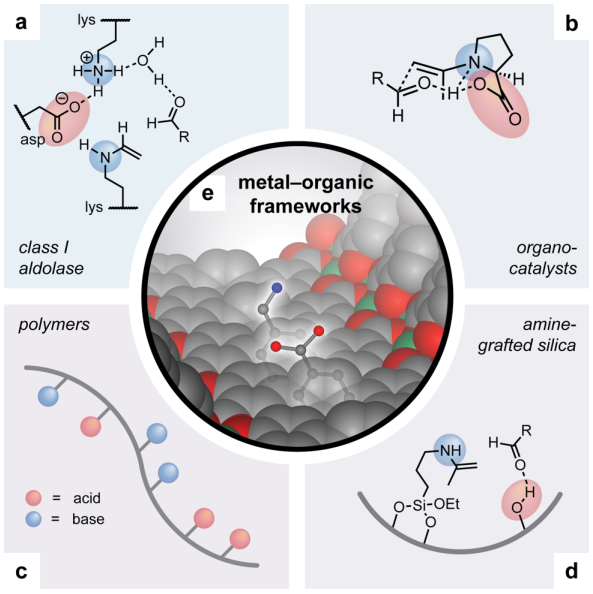

Figure 1. Overview of bifunctional acid–base catalysts for aldol condensation reactions, including (a) class I aldolase enzymes, (b) small molecule organocatalysts, (c) acid–base functionalized polymers, (d) amine-grafted mesoporous silica, and (e) metal–organic frameworks (*this work*). Figures a–d adapted from references 3, 6, 10, and 13, respectively.

Introduction.

In enzymes, multiple organic residues of moderate reactivity work together to facilitate heterolytic bond formation and cleavage under mild conditions. For example, class I aldolases use a combination of weakly acidic and basic residues to catalyze the aldol condensation (**Fig. 1a**). Conserved lysine and aspartate residues work cooperatively to generate the key enamine intermediate, all within a tightly hydrogen-bonded network that facilitates proton transfer and circumvents high-energy charged species.[1–3]

These lessons from biology have gained renewed relevance in the context of biomass utilization. Active sites in which the reactivity of the whole is greater than the sum of the individual parts provide significant stability and selectivity advantages. Weakly reactive functional groups are more resistant to poisoning by contaminants and less prone to unselective substrate polymerization and fouling, two of the most common catalyst

degradation pathways observed in biomass conversion technologies.[4,5]

Inspired by class I aldolases and other enzymes, bifunctional acid–base catalysts have been explored in multiple platforms, including small molecule amino acid and peptide catalysts (**Fig. 1b**),[6,7] functionalized organic polymers of both synthetic and biological origin (**Fig. 1c**),[8–11] and amine-grafted silica (**Fig. 1d**).[12–14] Clear cooperative effects have been observed in reactions relevant to biomass conversion, including the aldol condensation of biomass-derived methyl ketones into higher molecular weight biofuel precursors,[15] and the condensation of biomass-derived aldehydes (e.g., furfural, 5-hydroxymethylfurfural) into higher value products.[11,16]

Fully realizing the promise of enzyme-like cooperativity in a synthetic platform requires the ability to adjust active site parameters by as little as a few angstroms. In enzymes, the relative spatial rearrangement of amino acid residues is as critical to function as their number and identity. For example, lengthening the aspartate residue in a class I aldolase active site by just a single methylene unit dramatically reduces catalytic activity by over 40-fold.[1] This level of spatial precision is difficult, if not impossible, to replicate in supports such as amine-grafted mesoporous silica, where structural fidelity is fundamentally limited by the amorphous surface.

Given the importance of structural precision, we envisioned the use of metal–organic frameworks (MOFs) as a new platform for the construction of bifunctional acid–base active sites (**Fig. 1e**). The synthesis of Brønsted acid–base MOFs has received far less attention than its closely related counterpart, bifunctional Lewis acid–base MOFs.[17,18] While several examples of frameworks jointly functionalized with amine and sulfonic acid groups have been reported,[19,20] to our knowledge only one previous study has demonstrated the colocalization of carboxylic acids and amines in a single MOF pore.[21] In this prior work, the functional groups were post-synthetically incorporated in a single crystal-to-single crystal fashion using sequential linker installation. As this technique is specific to PCN-700, a zirconium-based framework containing an ordered array of missing linkers,[22] this study gained active site precision at the cost of generalizability and chemical tunability.

Here, we report a general strategy to template bifunctional acid–base sites in metal–organic framework pores. Using a mesoporous magnesium-based framework with ~3 nm pore channels, we show how carboxylic acid and benzylamine functional groups can be installed pairwise in a single configuration less than 7 Å apart. Relative to non-templated materials containing randomly distributed acid and base sites, the templated catalysts are over four-fold and two-fold more active for aldol condensation reactions with 4-nitrobenzaldehyde and furfural, respectively. Finally, the catalysts are stable and show no loss in activity or structural degradation after multiple cycles. Together, this work establishes metal–organic frameworks as an exciting platform for cooperative acid–base catalysis that balances the advantages of heterogeneous catalysts with the precision of enzymes.

Framework synthesis and characterization.

Our group has recently shown that thermolabile crosslinkers can be used to template pairs of functional groups in metal–organic framework pores at specific relative distances and orientations.[23,24] For example, we have used tertiary ester and tertiary carbamate-based crosslinkers to template pairs of carboxylic acids and pairs of amines in the terphenyl-expanded MOF-74 framework, also known as Mg_2dotpdc (dotpdc^{4-} = 4,4″-dioxido-[1,1′:4′,1″-terphenyl]-3,3″-dicarboxylate) (**Fig. 2a**). This framework contains large, one-dimensional hexagonal channels (~3 nm) framed by tightly packed ligand struts (~7 Å apart).[25–27] Mg_2dotpdc (abbreviated **1**) and other frameworks with similar 1D channels[28,29] are attractive supports for bifunctional

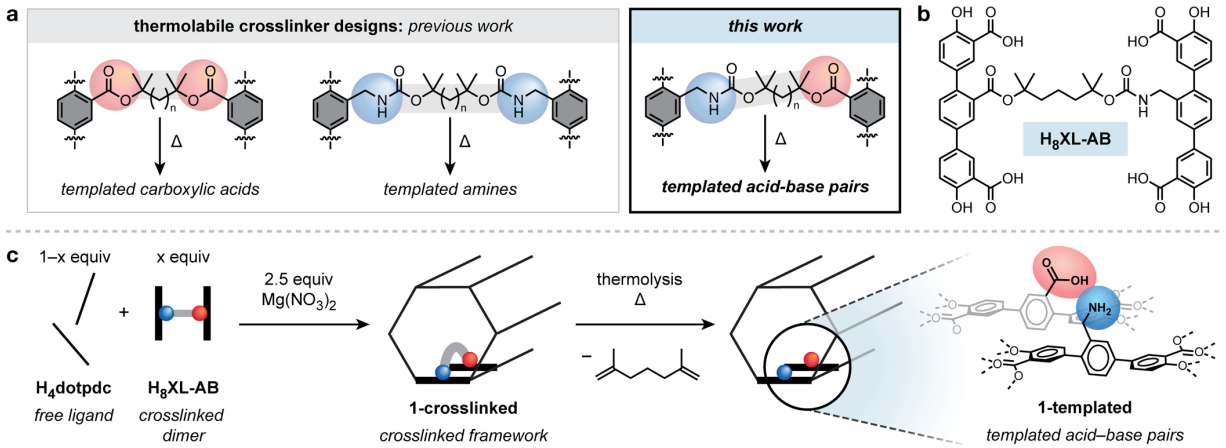

Figure 2. (a) Previous work on templating carboxylic acids and amines pairs (left) and templated acid–base pairs in this work (right). (b) Structure of the non-symmetric crosslinker featuring a tertiary ester and tertiary carbamate linkage. (c) Overview of our templating strategy where the non-symmetric crosslinker, **H8XL-AB**, is used to templated acid–base pairs.

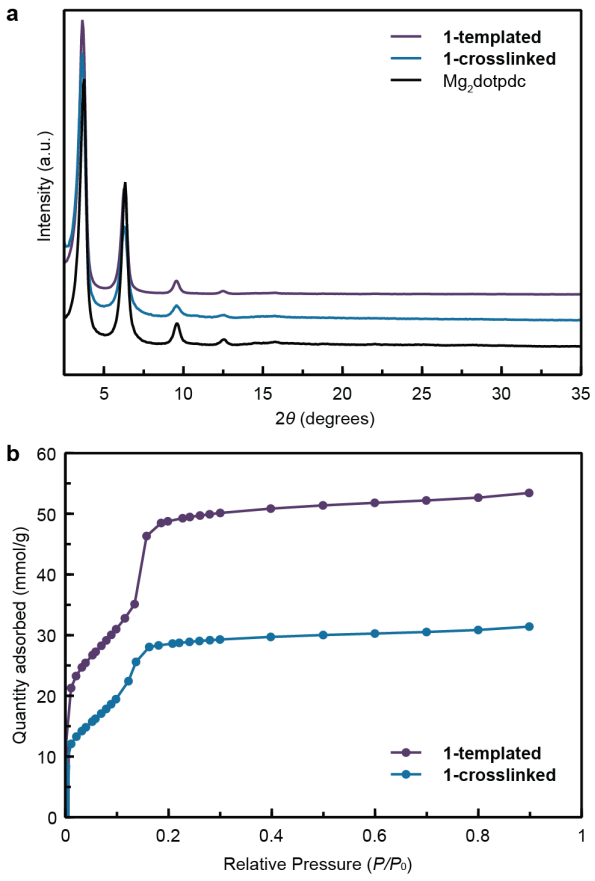

Figure 3. (a) Powder X-ray diffraction (PXRD) data of Mg_2dotpdc, **1-crosslinked**, and **1-templated** and (c) 77 K nitrogen adsorption data for **1-crosslinked** and **1-templated**.

catalysis, as they provide large pore diameters while still maintaining short distances between adjacent ligands.

To extend our templating strategy to bifunctional acid–base sites, we designed a new non-symmetric crosslinked ligand dimer, abbreviated **H8XL-AB**, which incorporates a tertiary ester linkage on one end and a tertiary carbamate linkage on the other. The two halves of the dimeric ligand are bridged by a short alkyl chain (**Fig. 2b**, see SI for synthetic details). After framework synthesis, thermal cleavage of the tertiary ester and carbamate groups should lead to bifunctional carboxylic acid and benzylamine pairs positioned on adjacent ligands roughly 7 Å apart (**Fig. 2c**).

The synthesis of the crosslinked Mg_2dotpdc framework, abbreviated **1-crosslinked**, was achieved by heating a mixture of the unfunctionalized ligand H_4dotpdc (0.875 equiv), crosslinked ligand dimer **H8XL-AB** (0.125 equiv), and $Mg(NO_3)_2$•$6H_2O$ (2.50 equiv) in a mixture of DMF and MeOH. After 3 h, a microcrystalline powder consistent with the Mg_2dotpdc structure was obtained (**Fig. 3a**). Digestion ^{1}H NMR analysis was used to quantify the framework composition and ensure no premature crosslinker degradation occurred during framework synthesis. We obtained a framework in which 24% of the ligands are crosslinked, which is slightly higher than

the expected incorporation of ~22% based on the ratio of the starting ligands (**Fig. S2**). The presence of the crosslinker peaks in the NMR (0.9 ppm–1.6 ppm) confirmed that no crosslinker degradation occurs under these conditions.

While there have been reports of separate tertiary carbamate[26,30] or tertiary ester[23] thermolysis in metal–organic frameworks, prior to this work the simultaneous cleavage of both groups within a single framework was not known. Excitingly, upon microwave heating at 230 °C, the mixed tertiary ester/carbamate crosslinker in **1-crosslinked** could be cleanly removed to generate **1-templated**, a framework containing acid and base pairs. Experimentally we have found that the primary amines in **1-templated** have heightened oxidative sensitivity due to the presence of neighboring acidic groups, and the microwave reaction must be done using samples that have been rigorously sparged and sealed under N_2.

Removal of the crosslinker is evident in the ^{1}H NMR of digested samples, which shows full disappearance of the crosslinker and the emergence of peaks associated with the carboxylic acid and benzylamine-functionalized ligands (abbreviated H_4dotpdc-CO_2H and H_4dotpdc-CH_2NH_2, **Fig. S3**). Together, the sum of H_4dotpdc-CO_2H (12%) and H_4dotpdc-CH_2NH_2 (10%) in the templated sample is roughly consistent with the number of crosslinked ligands in **1-crosslinked** (24%). We attribute the slight discrepancy (~2%) to the partial oxidation of the benzylamines during thermolysis. Carrying out the microwave reaction under air, rather than N_2, further reduces the H_4dotpdc-CH_2NH_2 percentage and introduces new features associated with aldehyde functional groups, supporting this hypothesis (**Fig. S4)**.

No structural degradation following thermal treatment is observed, as is evident by the powder X-ray diffraction (PXRD) patterns (**Fig. 3a**). A large increase in the Brunauer–Emmett–Teller (BET) surface area is observed, from 2130 m^2/g in **1-crosslinked** to 2730 m^2/g in **1-templated** (**Fig. 3b**). This latter value is within the range of previously reported surface areas for unfunctionalized Mg_2dotpdc (2440–3100 m^2/g), consistent with full removal of the crosslinker.[23,25,27]

Cooperative aldol condensation.

We next probed the ability of our templated frameworks to catalyze aldol condensation reactions (**Scheme 1**). We hypothesized that the amine could form a nucleophilic enamine intermediate, while the acid could participate in hydrogen-bonding and electrophilic activation of the aldehyde partner. Similar mechanisms have been shown in other bifunctional acid–base catalysts (**Fig. 1**).[6,31]

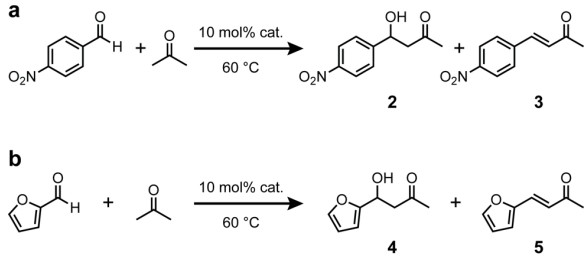

Scheme 1. Aldol condensation reactions with acetone and (a) 4-nitrobenzaldehyde and (b) furfural.

To provide unambiguous evidence of acid–base cooperativity, we synthesized four control frameworks: 1) **1-nontemplated**, a framework in which the acid and base groups are present in similar concentrations but are randomly distributed throughout the pores; 2) **1-CH_2NH_2**, a framework containing only amine groups; 3) **1-COOH**, a framework containing only carboxylic acid groups; and 4) **Mg_2dotpdc**, the bare framework containing no functional groups.

To synthesize the non-templated framework, we heated a mixture of H_4dotpdc-CO_2tBu (0.100 equiv), H_4dotpdc-CH_2NHBoc (0.100 equiv), H_4dotpdc (0.800 equiv), and $Mg(NO_3)_2$•$6H_2O$ (2.50 equiv) in DMF and MeOH for 3 h. Powder X-ray diffraction (PXRD) and ^{1}H NMR digestion

studies confirmed that the resulting framework, which contains protected carboxylic acid and benzylamine groups, adopts the desired Mg_2dotpdc structure (**Fig. S5**) with the expected functional group loading (~10% of each group, **Fig. S7**). The *tert*-butyl ester and carbamates in this framework were removed via microwave thermolysis to reveal **1-nontemplated** (**Fig. S6**). Like the templated framework, a large increase in BET surface area from 2440 m^2/g to 2780 m^2/g was observed upon thermolysis and removal of the protecting groups (**Fig. S8**). The control frameworks **1-CH_2NH_2** and **1-COOH** were synthesized in a similar fashion, but with functional group loadings of ~20 mol%.

Given how differences in particle size and internal mass transport limitations can obscure intrinsic differences catalytic activity, scanning electron microscopy (SEM) studies were carried out to confirm that all frameworks have similar morphologies. An average length of 0.307 ± 0.148 μm and an average diameter of 0.060 ± 0.018 μm was observed for **1-templated**, while an average length of 0.338 ± 0.139 μm and an average diameter of 0.077 ± 0.025 μm was obtained for **1-nontemplated** (**Figs. S9** and **S10**). These lengths and diameters are all within error of each other, confirming that the use of crosslinked ligand dimers at these concentrations has little impact on the resulting framework morphology. Together, these analyses confirm that all frameworks are identical in terms of their overall structure, surface area, and particle morphology, and differ only in their functional group content and spatial distribution.

We first evaluated the ability of each framework to catalyze the aldol reaction between 4-nitrobenzaldeyde and acetone to yield products **2** and **3** (**Scheme 1a**). This reaction has been widely used to benchmark heterogenous bifunctional acid-base catalysts.[11–14] Initial control experiments using the unfunctionalized Mg_2dotpdc framework revealed highly variable background reactivity. We hypothesized that the coordinatively unsaturated magnesium sites in the framework may be acting as Lewis acid catalysts, with activity that is highly sensitive to the presence of trace water. Indeed, this background reaction was nearly completely quenched upon the addition of a small amount of water (2 vol%) in the solvent mixture (**Table 1**). Given these results, we adopted 2 vol% water in acetone as our default solvent for all subsequent catalytic runs.

Table 1. Catalytic performance of frameworks for the aldol condensation of 4-nitrobenzaldehyde and acetone.[a]

Framework	Conversion (%)[e]
Mg_2dotpdc[b]	4
1-COOH[c]	11
1-CH_2NH_2[d]	25
1-nontemplated[d]	41
1-templated[d]	82

[a] All reactions were heated at 60 °C for 5 h in a water/acetone (2% v/v) with 0.05 M 4-nitrobenzaldehyde and 0.025 M of the internal standard 1,3,5-trimethoxybenzene.
[b] A catalyst loading: 30 mg
[c] A catalyst loading: 10 mol% (based on carboxylic acid content)
[d] A catalyst loading: 10 mol% (based on benzylamine content)
[e] Determined by ^{1}H NMR analysis.

We next compared the performance of each framework by monitoring substrate conversion after 5 h at 60 °C. The results, which are summarized in **Table 1**, show that **1-templated** achieves the highest conversion under these conditions (82%), followed by **1-nontemplated** with 41%

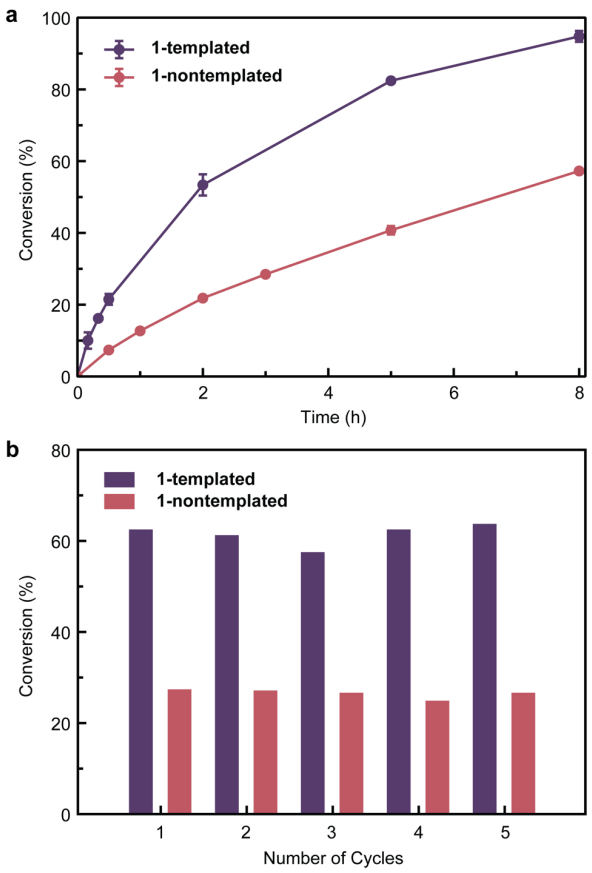

Figure 4. (a) Conversion of 4-nitrobenzaldeyhe in the aldol reaction with acetone over 8 h for **1-templated** and **1-nontemplated** catalysts. (b) Conversion of 4-nitrobenzaldehyde using the same samples of **1-templated** and **1-nontemplated** catalysts for five cycles at 60 °C for 3 h.

conversion. Both frameworks outperform the monofunctionalized **1-COOH** and **1-CH_2NH_2**, which achieve only 11% and 25% conversion, respectively. These initial catalyst screenings provide strong evidence that not only is the presence of both acid and base critical to activity, but also their spatial distribution.

To gain greater insight into the catalytic performance of **1-templated** and **1-nontemplated**, we monitored the kinetics of each reaction to obtain initial rates. Using the same conditions as before, timepoints ranging from 10 min to 8 h were collected in triplicate. At low conversion (<10%), initial turnover frequency (TOF) values of 6.26 and 1.49 h^{-1} were obtained for **1-templated** and **1-nontemplated**, respectively, indicating that the templated framework is over four-fold more active than the non-templated framework (**Fig. 4a**). Both catalysts are highly selective for the addition product **2** over the dehydrated product **3**. After 8 h, **1-templated** achieves 95% conversion (10:1 ratio of **2**:**3**), whereas **1-nontemplated** achieves 57% conversion (23:1 ratio of **2**:**3**). Both catalysts retain crystallinity over the 8 h period (**Fig. S11**), and digestion ^{1}H NMR of the frameworks confirms that both catalysts maintain the same functional group composition (**Figs. S12** and **S13**).

To test the stability and recyclability of **1-templated** and **1-nontemplated**, we performed cycling studies under the same catalytic conditions. After 3 h, the materials were washed with acetone and re-subjected to the reaction conditions (see **SI**). Both catalysts remain stable over five cycles, showing little variation in yields (**Fig. 4b**), no loss in crystallinity (**Fig. S14**), and no change in functional group composition (**Figs. S15** and **S16**).

In both frameworks, a small amount of 4-nitrobenzaldehyde is detected in the pores by ^{1}H NMR digestion studies even after rigorous washing with acetone. After one 8 h run, we detect 0.2–0.3 equiv of 4-nitrobenzaldehyde relative to the benzylamine loading **(Figs. S12** and **S13**). After five cycles, this value increased slightly to 0.4–0.6 equiv (**Figs. S15** and **S16**). We hypothesize that the aldehyde substrate may be reacting with our amines to form an off-cycle imine intermediate, which not only restricts access to the pores but also prevents the formation of the desired enamine. Substrate inhibition due to imine formation and pore clogging has been previously observed in primary amine-functionalized mesoporous silica, and is especially pronounced when the pore diameters are less than 3 nm.[32] The formation of off-cycle imines may explain why the initial four-fold difference in activity between **1-templated** and **1-nontemplated** appears to decrease over

longer reaction times. Future work will explore the use of secondary amine sites, which are not able to form stable imines.

Excitingly, evidence of cooperative catalysis is also observed when furfural, a biomass-derived aldehyde, is used as a substrate. We tested the performance of **1-nontemplated** and **1-templated** for the reaction between furfural and acetone, and the reaction was monitored for 16 h at 60 °C. (**Scheme 1b**). The results summarized in **Table 2** show that **1-templated** is a more active catalyst for this reaction, achieving a conversion of 72% (1:1.5 ratio of **4**:**5**) compared to 34% conversion (2:1 ratio of **4**:**5**) from **1-nontemplated**. Both frameworks remain crystalline, indicating that they are stable over 16 h (**Fig. S17**). These results, combined with the apparent stability over multiple cycles, demonstrates that MOFs with co-localized Brønsted acid and base groups serve as a promising catalyst for the conversion of biomass-derived aldehydes.

Table 2. Catalytic performance of frameworks for the aldol condensation of furfural and acetone.[a]

Framework	Conversion (%)[c]
1-nontemplated[b]	34
1-templated[b]	72

[a] All reactions were heated at 60 °C for 16 h in a water/acetone (2% v/v) with 0.05 M furfural and 0.025 M of the internal standard 1,3,5-trimethoxybenzene.
[b] A catalyst loading: 10 mol% (based on benzylamine content)
[c] Determined by ^{1}H NMR analysis.

Conclusion.

In summary, our work establishes a new route to achieve structurally unambiguous acid–base sites in a metal–organic framework. Significant cooperative effects are observed due to the colocalization of acid and base sites, with the templated materials catalyzing aldol condensation reactions up to four-fold faster than non-templated controls.

With the initial thermolabile crosslinker design now established, future catalyst modifications are limited only by our ability to synthesize slight variations of this underlying motif. Going forward, it should be straightforward to alter the identity of the templated functional groups to increase activity, such as changing the primary amine to a secondary amine. Work along this vein is under way. One can further imagine shortening the distance between acid–base pairs by replacing the benzylamine groups with a longer phenylethylamine, or, conversely, lengthening the distance by extending the crosslinker. As spatial precision is critical to harnessing cooperative interactions, we anticipate that these subtle adjustments will have dramatic effects on catalytic activity. Finally, given the orthogonal post-synthetic reactivity of carboxylic acids and amines, our templated sites can serve as a convenient and versatile entry point to more complex active sites, beyond simple acid–base pairs.

Acknowledgements

This material is based upon work supported by the National Science Foundation (NSF) under Grant No. 2142798. D.S.R. was supported in part by the state of Washington through a graduate fellowship from the University of Washington Clean Energy Institute. The authors acknowledge the use of instrumentation from the Molecular Analysis Facility, a National Nanotechnology Coordinated Infrastructure (NNCI) site at the University of Washington, which is supported in part by funds from the National Science Foundation (awards NNCI-2025489, NNCI-1542101), the

University of Washington, the Molecular Engineering & Sciences Institute, and the Clean Energy Institute. The authors gratefully acknowledge use of facilities and instrumentation supported by the U.S. National Science Foundation through the UW Molecular Engineering Materials Center (MEM-C), a Materials Research Science and Engineering Center (DMR-2308979). The NMR facility at the UW Department of Chemistry is supported by NIH Award Number S10OD030224-01A1.

References.

(1) Heine, A.; DeSantis, G.; Luz, J. G.; Mitchell, M.; Wong, C.-H.; Wilson, I. A. Observation of Covalent Intermediates in an Enzyme Mechanism at Atomic Resolution. *Science* **2001**, *294* (5541), 369–374. https://doi.org/10.1126/science.1063601.

(2) Frey, P. A.; Hegeman, A. D. *Enzymatic Reaction Mechanisms*; Oxford University Press: Oxford ; New York, 2007.

(3) Weiss, H. M. The Roles of Acids and Bases in Enzyme Catalysis. *J. Chem. Educ.* **2007**, *84* (3), 440. https://doi.org/10.1021/ed084p440.

(4) Lin, F.; Xu, M.; Ramasamy, K. K.; Li, Z.; Klinger, J. L.; Schaidle, J. A.; Wang, H. Catalyst Deactivation and Its Mitigation during Catalytic Conversions of Biomass. *ACS Catal.* **2022**, *12* (21), 13555–13599. https://doi.org/10.1021/acscatal.2c02074.

(5) Walker, T. W.; Motagamwala, A. H.; Dumesic, J. A.; Huber, G. W. Fundamental Catalytic Challenges to Design Improved Biomass Conversion Technologies. *Journal of Catalysis* **2019**, *369*, 518–525. https://doi.org/10.1016/j.jcat.2018.11.028.

(6) List, B.; Lerner, R. A.; Barbas, C. F. Proline-Catalyzed Direct Asymmetric Aldol Reactions. *J. Am. Chem. Soc.* **2000**, *122* (10), 2395–2396. https://doi.org/10.1021/ja994280y.

(7) Metrano, A. J.; Chinn, A. J.; Shugrue, C. R.; Stone, E. A.; Kim, B.; Miller, S. J. Asymmetric Catalysis Mediated by Synthetic Peptides, Version 2.0: Expansion of Scope and Mechanisms. *Chem. Rev.* **2020**, *120* (20), 11479–11615. https://doi.org/10.1021/acs.chemrev.0c00523.

(8) Merino, E.; Verde-Sesto, E.; Maya, E. M.; Iglesias, M.; Sánchez, F.; Corma, A. Synthesis of Structured Porous Polymers with Acid and Basic Sites and Their Catalytic Application in Cascade-Type Reactions. *Chem. Mater.* **2013**, *25* (6), 981–988. https://doi.org/10.1021/cm400123d.

(9) Zhang, Y.; Li, B.; Ma, S. Dual Functionalization of Porous Aromatic Frameworks as a New Platform for Heterogeneous Cascade Catalysis. *Chem. Commun.* **2014**, *50* (62), 8507. https://doi.org/10.1039/C4CC04012K.

(10) Hoyt, C. B.; Lee, L.-C.; Cohen, A. E.; Weck, M.; Jones, C. W. Bifunctional Polymer Architectures for Cooperative Catalysis: Tunable Acid–Base Polymers for Aldol Condensation. *ChemCatChem* **2017**, *9* (1), 137–143. https://doi.org/10.1002/cctc.201601104.

(11) Ellebracht, N. C.; Jones, C. W. Optimized Cellulose Nanocrystal Organocatalysts Outperform Silica-Supported Analogues: Cooperativity, Selectivity, and Bifunctionality in Acid–Base Aldol Condensation Reactions. *ACS Catal.* **2019**, *9* (4), 3266–3277. https://doi.org/10.1021/acscatal.8b05180.

(12) Zeidan, R. K.; Davis, M. E. The Effect of Acid–Base Pairing on Catalysis: An Efficient Acid–Base Functionalized Catalyst for Aldol Condensation. *Journal of Catalysis* **2007**, *247* (2), 379–382. https://doi.org/10.1016/j.jcat.2007.02.005.

(13) Brunelli, N. A.; Venkatasubbaiah, K.; Jones, C. W. Cooperative Catalysis with Acid–Base Bifunctional Mesoporous Silica: Impact of Grafting and Co-Condensation Synthesis Methods

on Material Structure and Catalytic Properties. *Chem. Mater.* **2012**, *24* (13), 2433–2442. https://doi.org/10.1021/cm300753z.
(14) Brunelli, N. A.; Jones, C. W. Tuning Acid–Base Cooperativity to Create next Generation Silica-Supported Organocatalysts. *Journal of Catalysis* **2013**, *308*, 60–72. https://doi.org/10.1016/j.jcat.2013.05.022.
(15) Sankaranarayanapillai, S.; Sreekumar, S.; Gomes, J.; Grippo, A.; Arab, G. E.; Head-Gordon, M.; Toste, F. D.; Bell, A. T. Catalytic Upgrading of Biomass-Derived Methyl Ketones to Liquid Transportation Fuel Precursors by an Organocatalytic Approach. *Angew Chem Int Ed* **2015**, *54* (15), 4673–4677. https://doi.org/10.1002/anie.201412470.
(16) Chen, J.-Y.; Brunelli, N. A. Investigating the Impact of Microporosity of Aminosilica Catalysts in Aldol Condensation Reactions for Biomass Upgrading of 5-Hydroxymethylfurfural and Furfuraldehyde to Fuels. *Energy Fuels* **2021**, *35* (18), 14885–14893. https://doi.org/10.1021/acs.energyfuels.1c01934.
(17) Huang, Y.-B.; Liang, J.; Wang, X.-S.; Cao, R. Multifunctional Metal–Organic Framework Catalysts: Synergistic Catalysis and Tandem Reactions. *Chem. Soc. Rev.* **2017**, *46* (1), 126–157. https://doi.org/10.1039/C6CS00250A.
(18) Zhang, Y.; Huang, C.; Mi, L. Metal–Organic Frameworks as Acid- and/or Base-Functionalized Catalysts for Tandem Reactions. *Dalton Trans.* **2020**, *49* (42), 14723–14730. https://doi.org/10.1039/D0DT03025B.
(19) Li, B.; Zhang, Y.; Ma, D.; Li, L.; Li, G.; Li, G.; Shi, Z.; Feng, S. A Strategy toward Constructing a Bifunctionalized MOF Catalyst: Post-Synthetic Modification of MOFs on Organic Ligands and Coordinatively Unsaturated Metal Sites. *Chem. Commun.* **2012**, *48* (49), 6151. https://doi.org/10.1039/c2cc32384b.
(20) Liu, H.; Xi, F.-G.; Sun, W.; Yang, N.-N.; Gao, E.-Q. Amino- and Sulfo-Bifunctionalized Metal–Organic Frameworks: One-Pot Tandem Catalysis and the Catalytic Sites. *Inorg. Chem.* **2016**, *55* (12), 5753–5755. https://doi.org/10.1021/acs.inorgchem.6b01057.
(21) Hu, X.-J.; Li, Z.-X.; Xue, H.; Huang, X.; Cao, R.; Liu, T.-F. Designing a Bifunctional Brønsted Acid–Base Heterogeneous Catalyst Through Precise Installation of Ligands on Metal–Organic Frameworks. *CCS Chem.* **2020**, *2* (1), 616–622. https://doi.org/10.31635/ccschem.019.201900040.
(22) Yuan, S.; Lu, W.; Chen, Y.-P.; Zhang, Q.; Liu, T.-F.; Feng, D.; Wang, X.; Qin, J.; Zhou, H.-C. Sequential Linker Installation: Precise Placement of Functional Groups in Multivariate Metal–Organic Frameworks. *Journal of the American Chemical Society* **2015**, *137* (9), 3177–3180. https://doi.org/10.1021/ja512762r.
(23) Geary, J.; Wong, A. H.; Xiao, D. J. Thermolabile Cross-Linkers for Templating Precise Multicomponent Metal–Organic Framework Pores. *J. Am. Chem. Soc.* **2021**, *143* (27), 10317–10323. https://doi.org/10.1021/jacs.1c04030.
(24) Geary, J.; Aalto, J. P.; Xiao, D. J. *Modular Synthesis of Templated Bimetallic Sites in Metal–Organic Framework Pores*; preprint; Chemistry, 2023. https://doi.org/10.26434/chemrxiv-2023-njhwz.
(25) Deng, H.; Grunder, S.; Cordova, K. E.; Valente, C.; Furukawa, H.; Hmadeh, M.; Gandara, F.; Whalley, A. C.; Liu, Z.; Asahina, S.; Kazumori, H.; O'Keeffe, M.; Terasaki, O.; Stoddart, J. F.; Yaghi, O. M. Large-Pore Apertures in a Series of Metal-Organic Frameworks. *Science* **2012**, *336* (6084), 1018–1023. https://doi.org/10.1126/science.1220131.
(26) Fracaroli, A. M.; Furukawa, H.; Suzuki, M.; Dodd, M.; Okajima, S.; Gándara, F.; Reimer, J. A.; Yaghi, O. M. Metal–Organic Frameworks with Precisely Designed Interior for Carbon

Dioxide Capture in the Presence of Water. *J. Am. Chem. Soc.* **2014**, *136* (25), 8863–8866. https://doi.org/10.1021/ja503296c.

(27) Milner, P. J.; Martell, J. D.; Siegelman, R. L.; Gygi, D.; Weston, S. C.; Long, J. R. Overcoming Double-Step CO_2 Adsorption and Minimizing Water Co-Adsorption in Bulky Diamine-Appended Variants of Mg_2 (Dobpdc). *Chem. Sci.* **2018**, *9* (1), 160–174. https://doi.org/10.1039/C7SC04266C.

(28) Rosi, N. L.; Kim, J.; Eddaoudi, M.; Chen, B.; O'Keeffe, M.; Yaghi, O. M. Rod Packings and Metal−Organic Frameworks Constructed from Rod-Shaped Secondary Building Units. *J. Am. Chem. Soc.* **2005**, *127* (5), 1504–1518. https://doi.org/10.1021/ja045123o.

(29) Rollins, D. S.; Geary, J.; Wong, A. H.; Xiao, D. J. Stabilizing Large Pores in a Flexible Metal–Organic Framework *via* Chemical Cross-Linking. *Chem. Commun.* **2022**, *58* (88), 12361–12364. https://doi.org/10.1039/D2CC04829A.

(30) Lun, D. J.; Waterhouse, G. I. N.; Telfer, S. G. A General Thermolabile Protecting Group Strategy for Organocatalytic Metal−Organic Frameworks. *J. Am. Chem. Soc.* **2011**, *133* (15), 5806–5809. https://doi.org/10.1021/ja202223d.

(31) Collier, V. E.; Ellebracht, N. C.; Lindy, G. I.; Moschetta, E. G.; Jones, C. W. Kinetic and Mechanistic Examination of Acid–Base Bifunctional Aminosilica Catalysts in Aldol and Nitroaldol Condensations. *ACS Catal.* **2016**, *6* (1), 460–468. https://doi.org/10.1021/acscatal.5b02398.

(32) Kandel, K.; Althaus, S. M.; Peeraphatdit, C.; Kobayashi, T.; Trewyn, B. G.; Pruski, M.; Slowing, I. I. Substrate Inhibition in the Heterogeneous Catalyzed Aldol Condensation: A Mechanistic Study of Supported Organocatalysts. *Journal of Catalysis* **2012**, *291*, 63–68. https://doi.org/10.1016/j.jcat.2012.04.005.